Hydrogeology Journal
https://doi.org/10.1007/s10040-022-02555-9

PAPER

Use of microbial communities to assess the mixing of deep and shallow groundwater: case study from southern China

Traore Adiaratou[1] · Xumei Mao[1] · Liang Feng[1] · Zide Shi[1] · Yaqun Dong[1] · Jianqiao Ye[1]

Received: 5 August 2021 / Accepted: 4 October 2022
© The Author(s), under exclusive licence to International Association of Hydrogeologists 2022

Abstract

Proper assessment of mixing with shallow groundwater is key to understanding the state and hydrochemical composition of deep groundwater. Each tracer technique (hydrochemistry, isotopes, temperature, etc.) used to evaluate mixing has its own applicability and disadvantages. Microorganisms in groundwater record the environment they experience and respond quickly to environmental changes, making them potential tracers. Three groups of groundwater (nine samples) from three different hydrogeological conditions in a hydrothermal system in Suining (southern China) were selected and assessed as a case study. The three groups of groundwater have similar hydrochemical types, but the chemical compositions are different. Moreover, the deep warm groundwater experiences a temperature of 66.5–74.6 °C and a circulation depth of 1.93 km. Species-level operational taxonomic unit (OTU) classification and principal component analysis (PCA) were performed for the microorganisms. Although Proteobacteria and Cyanobacteria are dominant, the microbial communities are significantly different in the three groups of groundwater. Moreover, Firmicutes, Fusobacteria and Cyanobacteria are positively correlated with Na^+, SO_4^{2-}, Cl^- and F^-, as well as the corresponding OTUs at the species level. The ratio of geothermal water mixed with shallow groundwater is evaluated by water chemistry (Cl^-, SO_4^{2-} and Na^+) and the average value is 46.46%, while the mixing ratio evaluated by the microbial community is 44.68 and 43.71% at the phylum and species level, respectively. Similar assessment results indicate that the microbial community can be used as an effective tracer to estimate the mixing of deep geothermal water with shallow groundwater.

Keywords Micro-organisms · Hydrochemistry · Geothermal systems · Shallow groundwater · Tracers

Introduction

Characterization of groundwater mixing is an important hydrogeological problem, which can be used to explain the origin of groundwater chemical components, changes in pollutants and their concentrations in groundwater, and the original status of geothermal fluids (Xue et al. 2009; Al-Qudah et al. 2011). The original characteristics of deep geothermal fluid are the basis for correctly identifying geothermal systems and for science-based utilization of geothermal resources (Stefánsson et al. 2019). The characteristics of deep geothermal fluids are mostly interpreted from the exposed hot springs. However, hot springs do not always represent the deep geothermal fluids due to mixing with shallow groundwater. It is necessary to properly evaluate the degree of mixing with shallow groundwater in order to characterize the deep geothermal fluids (Fournier and Truesdell 1973; Han et al. 2010).

Many tracers, such as hydrochemicals, isotopes, temperature, etc., are used to assess the mixing of deep geothermal water with shallow groundwater (Girmay et al. 2015; Li et al. 2017). Different water–rock interactions form different hydrochemical components, which is the main principle in the use of hydrochemical indicators to evaluate groundwater mixing. However, similar water–rock interaction environments may make it difficult to use hydrochemical indicators for assessing groundwater mixing (Wang et al. 2021). Isotope fractionation and isotope exchange in flowing groundwater may also lead to the failure of isotope tracers to evaluate the degree of groundwater mixing (Modie et al. 2022). When studying geothermal water by temperature indicators, there may be misinterpretation in the assessment of groundwater mixing, due to adiabatic boiling and cooling and heat transfer

✉ Xumei Mao
maoxumei@cug.edu.cn

[1] School of Environmental Studies, China University of Geosciences, Wuhan 430074, China

Published online: 18 October 2022

during upward migration (Hou et al. 2019; Pérez-Zárate et al. 2022). The use of multiple tracers together is more reliable to assess the mixing of deep geothermal water and shallow groundwater (Aydin et al. 2020; Yuan et al. 2022).

Microorganisms have a good response to the groundwater environment (Haveman and Pedersen 2002). The temperature, pH, and salinity of groundwater can affect the chemical composition of groundwater and also dominate the types of microorganisms found in groundwater (Woolard and Irvine 1994; Holden et al. 1998; Křoupalová et al. 2013). The microbial community structure may be significantly different in geothermal and ambient temperature groundwater (Beyer et al. 2015). Microorganism communities present "fingerprints" that can indicate different sources of groundwater (Park et al. 2016; Zeng et al. 2016), making it possible to use them to assess groundwater mixing. Moreover, the timescale of the microbial community response to environmental changes is usually 10^0–10^1 years (Haack et al. 2004; Zhou et al. 2012), and the microbial communities can change over a period of even a month with environmental changes and still keep the same microbial species (Mu et al. 2021). However, the chemistry of deep groundwater, as the result of water–rock interaction, usually has a long response time to environmental changes (10^3–10^4 years), and this may cause the results of a mixing assessment to deviate due to the delayed response of the water chemistry to mixing (Birkle et al. 2009; Wu et al. 2020). Thus, microbial community structure is expected to be another suitable tracer for assessing groundwater mixing (Hallbeck and Pedersen 2011; Ye et al. 2016).

Silica-enriched groundwater, resulting from the exposure of groundwater to the granite fracture network, is abundant and widely distributed in Suining, South China. In this area, there is a commercial use for mineral drinking water. Geothermal activity and the weathered granite fracture network promote the occurrence of high-concentration soluble silica in groundwater (>40 mg/L). These hydrogeological conditions, groundwater flow processes and hydrochemical mechanisms have been discussed in Mao et al. (2022). This paper describes the estimation of the degree of mixing of geothermal water and shallow groundwater using hydrochemical indicators and microbiological indicators, in an attempt to determine the feasibility of using microbial community structure as a new tracer.

Study area

The study area is located in the north of Suining County, southeast of Hunan Province, in southern China. The area has a subtropical monsoon climate, with an average annual temperature of 16.7 °C. The maximum temperature is in July (27.2 °C), and the minimum temperature is in January (–4 °C). The average annual precipitation in the study area is 1,356.2 mm; from April to August the average precipitation is 857 mm, and from January to December the average precipitation is 163.7 mm.

Magmatic intrusion occurred in multiple periods of geological history, forming widely distributed granites in the study area (Xie et al. 2010). These granitic rocks had experienced many stages of geological tectonic activity and formed fault zones. The broken granite in the fault zone is weathered in the shallow surface layer. The Indosinian granites are the most extensive outcrop bedrock. The Quaternary strata are widely distributed in the gully areas, which are formed by weathering granite and consist of clay and gravel layers.

Three sets of fractures, developed uniformly from shallow to deep, were formed by the condensation of magmatic rocks after intrusion. The three groups of fractures include (1) strike direction of 330°, inclination of SW, inclination angle of 70°, 2–3 fractures/m; (2) strike direction of 280°, inclination of S, inclination angle of 80°, 2 fractures/m; (3) strike direction of 260°, inclination of N, inclination angle of 55°, 2 fractures/m. The three groups of fractures in the granite area of the study area combine with each other to form a fracture network. The study area has developed a north–south main fault (F86) and many secondary faults, which are affected by multistage geological tectonic activities. The formation of F86 may have been in the Indosinian period, but the obvious activity in the Yanshan period indicates that it is a long-term active fault zone. At the southern end of F86, there is a secondary fault, F86-1, with similar characteristics to the main fault in the study area (Fig. 1). The radioactive elements in granite such as uranium (U) and thorium (Th) can generate radioactive heat and cause the temperature of groundwater to rise (Li et al. 2017). Furthermore, the main fault zone (F86), being subjected to multiple activities, caused the granite body to strike-slip. Frictional heating, caused by fault zone motion, provides additional heat to the hot springs of F86 and F86-1, in addition to normal geothermal warming (Tang et al. 2017).

Two aquifer groups can be recognized in the studied area. The pore-water aquifer is constituted by Quaternary strata with coarse-medium sands and gravel, and the fracture-water aquifer is comprised of Indosinian granites. Furthermore, the extensively developed fracture network is a channel for groundwater storage and migration. Mountain valleys are mostly formed along the main fault zone (F86), and the accompanying secondary faults are favorable sites for groundwater gathering. The secondary fault (F86-1) is a structure associated with water-bearing strata, water catchment characteristics and water conduction on the west side of the study area, but it blocks water on the east side. The groundwater in the area is mainly recharged by atmospheric precipitation in origin, flows from west to east through the fault zone and the granite fracture network, and eventually discharges into the stream in the form of springs.

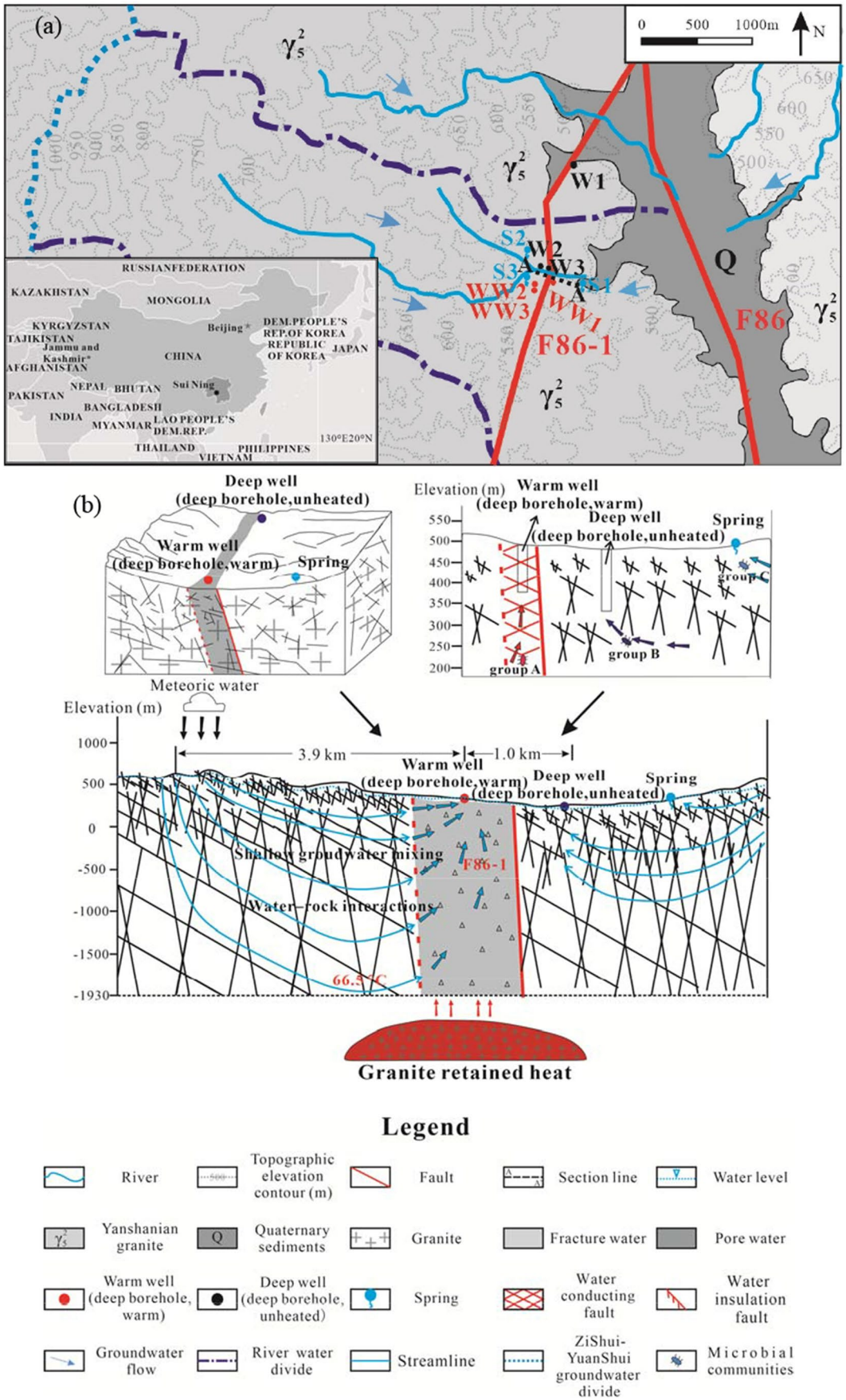

Fig. 1 **a** Sampling locations and faults. **b** Flow processes of the three groups of groundwater (A, B, C) in the granite fracture network

Sampling and analysis methods

According to hydrogeological conditions, F86-1 is an anisotropic fracture collecting and conducting water on the west side of the study area, and it is connected with the granite fracture network. Due to the adequate ground-survey, borehole and hydrogeological observations, the hydrogeological conditions in the study area are well characterized (Mao et al. 2022). Samples for microbial analysis were taken from nine locations: three deep warm-water boreholes, three boreholes representing deep unheated groundwater, and three springs. Microbial samples were not collected from borehole W4, described in Mao et al. (2022), due to the mixing of shallow and deep groundwater in the borehole. The nine samples were divided into three groups, representing three different hydrogeological conditions:

- Deep warm groundwater, samples WW1, WW2, WW3 taken from F86-1, marked as group A. The microbial compositions of WW1, WW2 and WW3 were denoted as A1, A2 and A3, respectively.
- Deep unheated groundwater in the granite fracture network, samples W1, W2, W3 taken from both sides of F86-1, marked as group B. The microbial compositions of W1, W2 and W3 were denoted as B1, B2 and B3, respectively.
- Shallow groundwater (unheated), samples S1, S2, S3 flowing from the weathered surface of granite, marked as group C. The microbial compositions of S1, S2 and S3 were denoted as C1, C2 and C3, respectively.

Hydrogeochemistry

The samples from the boreholes were collected after pumping for half an hour and the spring samples were gathered from the exposed spring flow. All water samples to be analyzed for anions and cations were first filtered with 0.45-μm membranes, and then contained in polyethylene bottles washed by filtered water three times. In addition, the bottles used for cation analysis were filled and sealed with no bubbles, and the anion water samples were brought to pH <2 by the addition of ultrapure nitric acid.

The values of temperature, pH and electrical conductivity (EC) were measured in situ with a 5-Star multi-parameter water quality analyzer (520M-01 model). The alkalinity was determined by titration technique in the field and the precision was generally around ±0.5 mg/L. The main anions and cations were analyzed using the Dionex ion chromatograph (ICS1100 model) and an inductively coupled plasma spectrometer (ICP-OES, ICAP6300 model), respectively. The errors associated with anions and cations based on calculating the ion balance were ±2%, and the detection accuracy was about 0.001 mg/L. These analyses were undertaken in the laboratory of the Environmental School, China University of Geosciences (Wuhan). The hydrogeochemical results are listed in Table 1.

Table 1 Groundwater hydrochemical composition and microbial sampling analysis under three different hydrogeological conditions (groups A, B and C) from Suining, South China (unit: mg/L)

Group	Sample	Water	Well depth (m)	T (°C)	pH	EC (μS/cm)	Dissolved CO_2	HCO_3^-	Cl^-	NO_3^-	SO_4^{2-}	K^+	Na^+	Ca^{2+}	Mg^{2+}	SiO_2	Microorganism
A1	WW1	Warm well	200.6	20.1	7.25	120.19	19.72	82.81	1.134	1.675	2.257	1.117	8.672	19.438	1.120	43.23	DNA and species
A2	WW2	Warm well	198.8	19.6	7.23	142.32	21.66	90.96	4.569	0.269	4.495	1.404	9.642	23.822	0.942	51.57	DNA and species
A3	WW3	Warm well	100.4	18.1	7.14	128.97	19.52	81.98	5.214	0.000	5.934	1.860	8.412	21.156	1.790	43.51	DNA and species
B1	W1	Deep well	300.3	15.3	7.13	100.21	16.29	68.41	4.448	0.328	8.788	0.255	25.247	5.389	0.018	27.33	DNA and species
B2	W2	Well	100.2	16.0	7.12	97.18	11.12	46.69	8.467	1.171	5.383	4.778	10.055	10.765	0.562	32.47	DNA and species
B3	W3	Well	100.3	15.5	7.13	93.65	9.72	40.84	8.573	1.521	6.269	3.693	8.727	10.846	0.757	32.59	DNA and species
C1	S1	Spring	-	15.7	7.02	56.56	4.56	19.17	1.060	0.513	2.403	1.006	4.814	2.903	0.377	33.72	DNA and species
C2	S2	Spring	-	15.0	6.44	68.14	4.72	19.83	6.057	1.336	4.410	1.915	5.421	5.351	0.731	32.93	DNA and species
C3	S3	Spring	-	15.2	7.01	54.52	3.71	15.59	2.045	1.021	2.258	1.078	4.427	3.259	0.528	31.28	DNA and species

Microorganisms

Since each water sampler after being sterilized can only hold 2 L, three samplers were used for simultaneous sample collection at each sampling point. A total of 6 L of fresh groundwater sample were collected. Samples were filtered using six microporous membranes—diameter of 100 mm and an opening 0.22 m (Whatman, UK)—each of which filtered 1 L of water sample. Each bacterial biomass sample was frozen in 50-ml sterile centrifuge tubes and sent to the Geological Microbiology Laboratory, Chinese University of Geology (Wuhan) and stored at –80 °C for further analysis. Three samples of each group were collected, and repeated measurements were performed.

Total DNA was extracted using FastDNA SPIN Kits for Soil (MP Biomedical, USA). The hypervariable V4 region of the 16S rRNA gene was amplified with a universal primer set (515F:5'-GTGCCAGCMGCCGCGGTAA-3' and 806R:5'-GGACTACVSGGGTATCTAAT-3') and the PCR (polymerase chain reaction) conditions were consistent with the study by Wu et al. (2019). Conditions involved: 50-µl PCR reactions, containing 25-µl 2x Premix Taq (Takara Biotechnology, Dalian Co. Ltd., China), 3-µl DNA template, 1 µl each primer, and 20-µl Nuclease-free water. PCR conditions: initial denaturation carried out at 94 °C for 5 min, after which the denaturation cycle was performed 30 times, each time 30 s; the temperature of each annealing is 52 °C and the time is 30 s; the extension is performed at 72 °C for 30 s and cycle 30 times; the final extension is carried out at 72 °C for 10 min. The length and concentration of the PCR product were detected by 1% agarose gel electrophoresis, and samples with bright main bands between 290 and 310 bp could be used for further experiments. PCR amplification purification was done through the use of the AxyPrep DNA Gel Extraction Kit for high-throughput sequencing at Guangdong Magigene Biotechnology Co., Ltd. Guangzhou, China.

A total of 686,865 raw reads were obtained after filtering protocols; per sample, this ranged from 43,646 to 107,096 reads. Reads were clustered into species-level operational taxonomic units (OTUs) at 97% similarity using QIIME2 software (version 1.9.1). A table with the OTUs abundance of more than 0.001% of the total number of each sample and the taxonomic assignments for each OTU was built for further analysis. The microbial diversity and richness of each sample was estimated using the mothur version 1.35.1. R is a language and environment for statistical calculations and graphics, which provides a variety of statistical information and graphics technology (Song et al. 2020). The relationship between the physicochemical variables and the bacterial community structure was analyzed using the vegan package in R version 4.0.2.

Geochemical computations

The reaction equilibrium between geothermal water and surrounding rock is reached, and the content of hydrochemical components is positively correlated with temperature. The heat exchange temperature of deep geothermal water can be evaluated according to geothermal water chemistry. This is the basic principle of the water chemical geothermometers (Fournier and Truesdell 1973; Fournier 1977). These hydrochemical geothermometers include SiO_2-quartz, SiO_2-chalcedony and cations (K, Na, Ca, Mg, Li, etc.; Fournier and Truesdell 1973; Fournier 1977; Arnórsson et al. 1983; Giggenbach et al. 1983; Nieva and Nieva 1987). The circulation depth of geothermal water can be evaluated based on geothermal temperature. (Mao et al. 2018):

$$D = \left(T - T_0\right)/G + Z_0 \tag{1}$$

where D is the circulation depth (m); T is the estimated reservoir equilibrium temperature (°C); T_0 is the local annual temperature (°C); G is the thermal gradient (°C/ m) and Z_0 is the thickness of the constant temperature zone (m).

The silica-enthalpy mixing model can be used to evaluate the mixing ratio of deep and shallow groundwater, but it is unsuitable for low-temperature hydrothermal systems (Fournier 1977). The effect of hydrochemistry on the content of chloride ions (Cl^-) in groundwater is minor and Cl^- can be used as a mixed indicator for deep groundwater and shallow groundwater (Han et al. 2010). Geothermal groundwater will mix with shallow groundwater as it migrates upwards. A stable tracer is used to evaluate the mixing of geothermal groundwater and shallow groundwater, which can be expressed as:

$$R_S X + R_R(1 - X) = R_{Mix} \tag{2}$$

where X is the mixing proportion, R_R is a certain stable tracer content in real deep warm groundwater, R_S is a certain stable tracer content in shallow groundwater, and R_{Mix} is a certain stable tracer content in mixed groundwater.

The mineral saturation index (SI) can be used to describe the supersaturation or undersaturation of different minerals' dissolution in groundwater systems, calculated by the hydrogeochemical modeling software PHREEQC (Parkhurst and Appelo 1999; Qin et al. 2005). When the estimated mineral saturation index is less than 0, this indicates that the balance between water and rock interaction in the groundwater system is insufficient at the measured temperature. PHREEQC can also be used to predict the mineral composition resulting from water–rock interaction according to the water chemical components (Plummer 1985). According to the predicted mineral composition and geothermal temperatures, it is possible to estimate the chemical composition of deep geothermal water.

Results and discussion

Hydrochemical characteristics and groundwater environment

The three groups of groundwater have similar hydrochemical characteristics, in that they are rich in silica and dominated by HCO_3^-, Na^+, Ca^{2+}. The hydrochemical types are basically HCO_3–Na+Ca and HCO_3–Na type. However, the concentrations of various ions in the three groups of groundwater are different because of the different hydrogeological conditions.

The deep warm groundwater has the highest concentrations of HCO_3^-, Ca^{2+}, and dissolved SiO_2 among the three groups of groundwater, which may be related to the strong mineral dissolution occurring in the warm groundwater environment (Stelling et al. 2016). However, the deep unheated groundwater has higher Na^+ content than the deep warm groundwater, which may be due to the ion exchange of Na–Mg and Na–Ca in groundwater circulation resulting in low content of Mg and Ca in the deep groundwater (Chae et al. 2006). The spring water has low contents of EC, HCO_3^-, Na^+ and Ca^{2+}, which may represent the insufficient water–rock interaction in shallow groundwater (Li et al. 2017). The deep warm groundwater has higher dissolved SiO_2 content, which may be related to geothermal activity. The water–rock interactions determine the water chemistry environment of the groundwater in which the microbial communities live.

The granite fracture network is connected to the faults, which provide groundwater accumulation space and migration channels (Song et al. 2016). Regional deep faults can connect shallow and deep groundwater, and can also provide convenient channels for geothermal flow (Marbun et al. 2020). According to hydrogeological conditions, it can be speculated that the F86-1 deep fault may transmit deep geothermal flow and provide the possibility for groundwater heating. On the west side of F86-1, there is a regional watershed (Zishui-Yuanshui Watershed) which is regarded as a groundwater recharge area. The lateral distance from the watershed to F86-1 is approximately 3.90 km.

According to the hydrogeological conditions of the study area, the chalcedony (maximum steam loss) and Na–K–Ca–Mg geothermometers are suitable for medium-low temperature hydrothermal systems in South China (Ndikubwimana et al. 2020; Mao et al. 2021). Considering that geothermal water may mix with shallow groundwater during the upward migration process (Mao et al. 2015), the estimated temperature of 66.5–74.6 °C is appropriate. Substituting the constant temperature zone thickness of 0 m (Yang et al., 2017) and the thermal gradient of 0.03 °C/m (Yuan et al. 2006) into Eq. (1), the maximum circulation depth of the deep warm groundwater is calculated to reach 1.93 km.

The three groups of groundwater are associated with differences in hydrogeology and hydrogeochemistry, which indicates that they have experienced different groundwater circulation processes (Fig. 1). The deep warm groundwater is recharged by meteoric water, and the groundwater infiltrates in the granite fracture network to a depth of 1.93 km and is heated to 66.5–74.6 °C, converging and discharging in the F86-1 fault zone. The deep unheated groundwater is also recharged by meteoric water, and migrates to a certain depth in the granite fracture network and is finally discharged into streams. The shallow groundwater is recharged by meteoric water and flows in the shallow granite fracture network. Thus, the three groups of groundwater, representing respective hydrogeological conditions, have different groundwater environments and different microbial communities.

Microbial communities in different groundwater environments

The microbial communities are represented in a stacked histogram (Fig. 2). Group A (A1, A2, A3) represents bacterial communities in deep warm groundwater, group B (B1, B2, B3) represents them in deep unheated groundwater, and group C (C1, C2, C3) represents them in shallow groundwater.

The phylum level is helpful to understand the dominant species of microbial communities in different groundwater environments, so the phylum level is selected for relative abundance statistics. The counted number is the same when calculating the relative abundance of the microbial communities, indicating that the relative abundance represents the absolute number of the microbial communities. The relative abundances of the main microbial communities in groups A, B, and C are different—for example, the relative abundance of Proteobacteria in groundwater group A is about 74%, which is significantly higher than that in groups B and C (60%, 45%). In addition, the microbial communities with a relative abundance of 2–10% in group C are completely different from those in groups A and B. The relative abundance of the Bacteroidetes that generally live in a parthenogenic aerobic groundwater environment in group C is about 18%, higher than in groups A and B (9 and 10%). The relative abundance of Actinobacteria, Firmicutes and Fusobacteria and Cyanbacteria living in the deep groundwater environment in group B is about 9, 3, 4 and 5%, respectively, which are higher than other groups. In addition, the relative abundance of Verrucomicrobia, Planctomycetes, and Acidobacteria in group C is above 2%, which is much more than that in other groups. Combining the microbial community composition and the relative abundance of different microbial communities, the microbial community composition of deep warm groundwater is slightly different from that of deep groundwater, while the microbial community composition of shallow groundwater is quite different from the others.

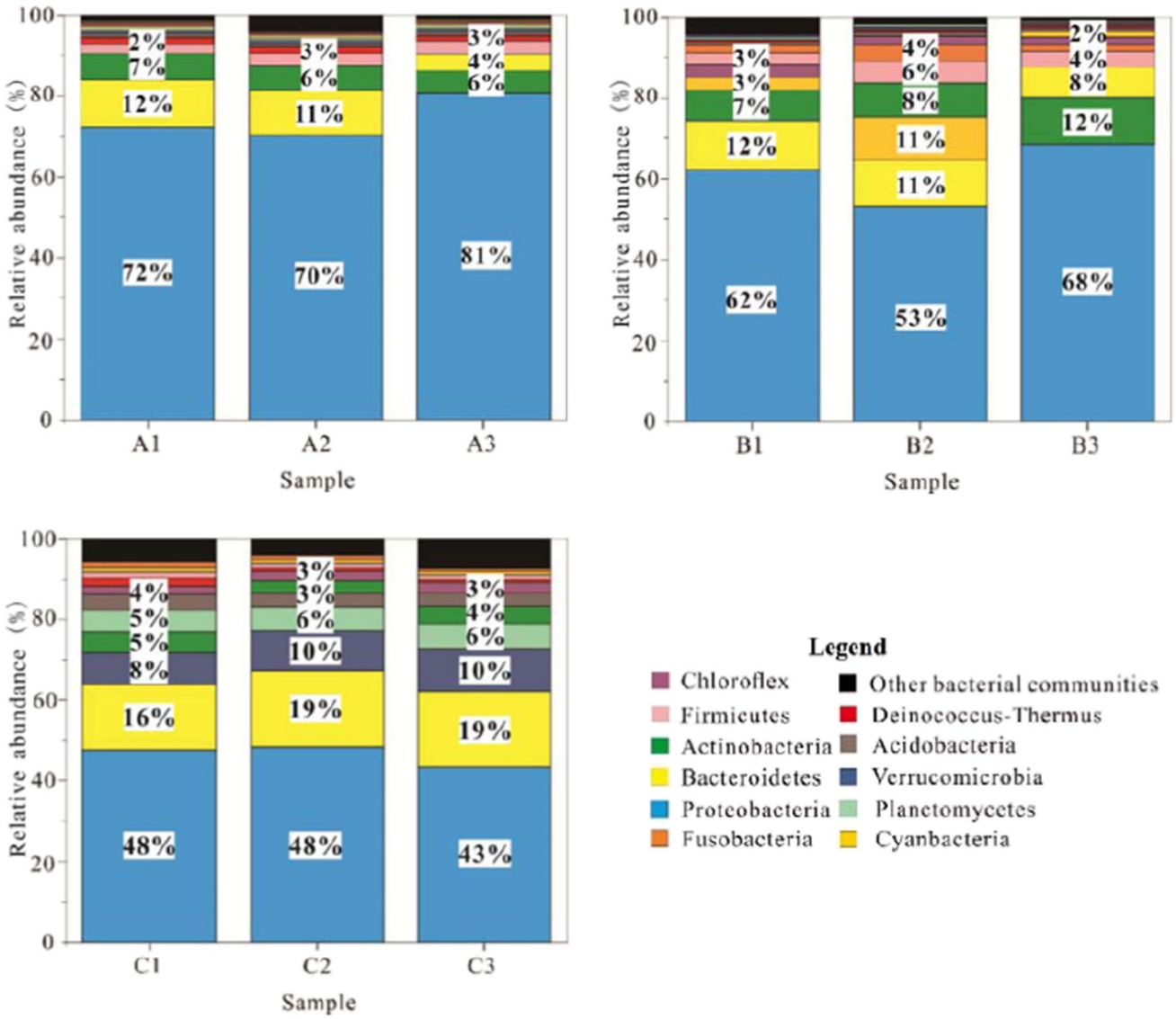

Fig. 2 Percentages of relative abundance of microbial communities in groundwater samples from Suining, South China

In accordance with the OTU representative sequence of the test results, taxonomic analysis is performed to obtain the bacterial community composition of three groups. The relative abundance of the microbial communities in the three groups A, B, C can be used to distinguish the difference in the bacterial communities in the groundwater environments. The results showed that the detected OTU mainly belonged to 26 categories. Principal component analysis (PCA) is performed on nine groups of microbial communities to distinguish the microbial community structure (Fig. 3). PC1 (63.79%) and PC2 (17.34%) could explain 81.13% of these nine variables, which means that the principal component analysis is reliable. The positions of groups A and B are relatively close and this indicates that the microbial community structure of deep warm groundwater and deep unheated groundwater is partially similar. In contrast, the position of group C being farther from the other groups indicates that the microbial community in shallow groundwater is quite different from that in the deep groundwater environments (groups A and B).

The Statistical Product and Service Solutions (SPSS) software is widely used to analyze the correlation between data. SPSS 17.0 was used to analyze the bivariate correlation with the Pearson correlation coefficient between the relative abundance of microbial communities and water chemistry data. Through software analysis, the correlations between microbial communities with relative abundances greater than 2% in groundwaters A, B and C and the main elements of water chemistry are obtained (Table 2). The histogram of water chemical content is compared with the histogram

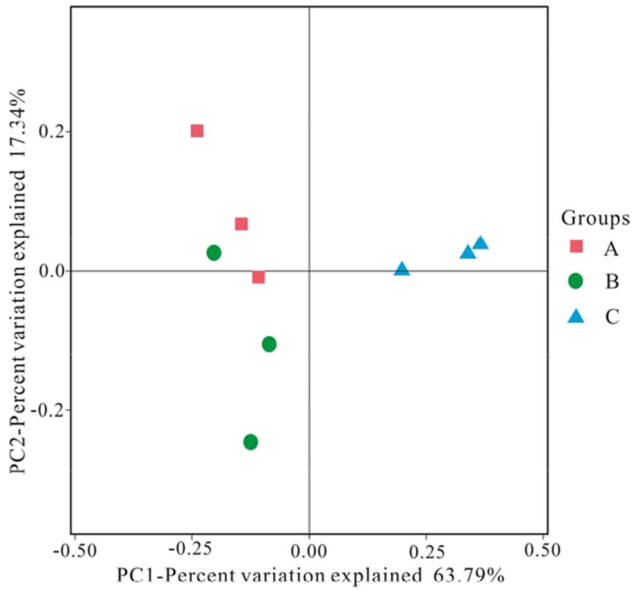

Fig. 3 Principal component (PC) analysis of the microbial communities (phylum level) in groundwater samples from Suining, South China

of the relative abundance of microorganisms to show the status of the two factors in different groundwater environments (Fig. 4). The Proteobacteria is the largest category and includes facultative or obligate anaerobic microorganisms that live an autotrophic or heterotrophic life (Stackebrandt et al. 1988; Guo et al. 2019). Proteobacteria presence is positively correlated with groundwater temperature ($R^2 = 0.757$), and Ca^{2+} and HCO_3^- content, indicating that the number of Proteobacteria would be relatively high when the corresponding values of physical and chemical parameters associated with the groundwater in the study area are high. The sufficient water–rock interaction in the deep warm groundwater, which has been in deep circulation and heated by granite that has retained heat at the fault, leads to higher Ca^{2+} and HCO_3^- contents in the warm-water boreholes than in other samples. The relative abundance of Proteobacteria in group A (deep warm groundwater) is higher than that in group B (deep unheated groundwater) and group C (shallow groundwater), indicating the corresponding relationship between Proteobacteria and the deep warm groundwater environment in the study area. Firmicutes and Fusobacteria are positively correlated with the content of Na, SO_4^{2-} and Cl^- in groundwater ($R^2 > 0.67$), while the water chemistry environment of deep unheated groundwater (group B) has a high content of the corresponding ions (Na, SO_4^{2-} and Cl^-) due to ion exchange and water–rock interactions. This implies that these two microbial species of Firmicutes and Fusobacteria are biased to survive in deep unheated groundwater (group B). Similar to Firmicutes and Fusobacteria, the relative abundance of Cyanobacteria is the largest in

Table 2 Correlation between microbial communities and hydrochemical characteristics of the groundwater samples from Suining, China (unit: mg/L)

Sample	T	pH	EC	HCO_3^-	F^-	Cl^-	SO_4^{2-}	NO_3^-	K^+	Na^+	Ca^{2+}	Mg^{2+}	SiO_2
Acidobacteria	−0.399	−.827**	−.932**	−.959**	−0.479	−0.54	−0.507	−0.351	0.42	−0.665	−0.583	−0.163	−0.078
Actinobacteria	−0.166	0.321	0.5	0.565	.775*	.800**	.787*	−0.21	−.748*	.842**	0.019	−0.37	−0.436
Bacteroidetes	−0.479	−.786*	−.842**	−.851**	−0.272	−0.329	−0.298	−0.442	0.217	−0.45	−0.619	−0.29	−0.22
Chloroflexi	−.675*	−0.427	−0.278	−0.214	0.614	0.586	0.602	−.687*	−0.638	0.511	−0.604	−.718*	−.722*
Cyanobacteria	−0.439	−0.117	0.034	0.094	0.635	0.629	0.633	−0.463	−0.639	0.603	−0.33	−0.54	−0.568
Deinococcus–Thermus	0.459	0.588	0.586	0.577	0.019	0.06	0.038	0.439	0.021	0.153	0.528	0.353	0.311
Firmicutes	−0.011	0.433	0.583	0.635	0.656	.689*	.671*	−0.054	−0.622	.750*	0.163	−0.213	−0.279
Fusobacteria	−0.371	0.03	0.2	0.265	.725*	.729*	.727*	−0.403	−.717*	.725*	−0.228	−0.514	−0.557
Planctomycetes	−0.491	−.878**	−.959**	−.977**	−0.385	−0.448	−0.414	−0.446	0.323	−0.582	−0.663	−0.264	−0.181
Proteobacteria	.757*	.930**	.915**	.895**	−0.026	0.04	0.004	.728*	0.089	0.187	.855**	0.599	0.536
Verrucomicrobia	−0.449	−0.854**	−0.947**	−0.969**	−0.433	0.342	−0.449	−0.403	0.383	−0.621	−0.597	−0.209	−0.135

*The correlation is significant at the 0.05 level, **the correlation is significant at the 0.01 level

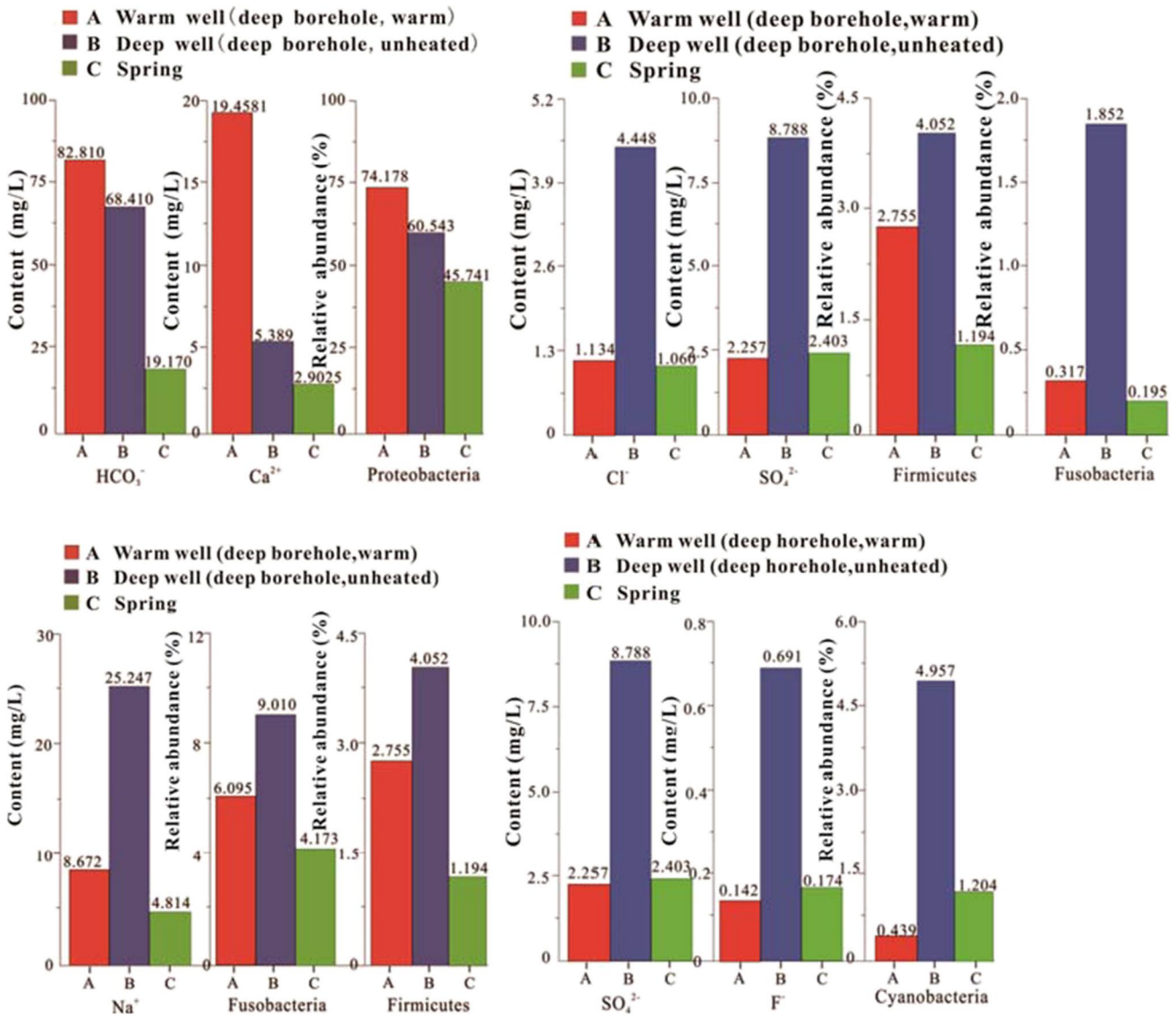

Fig. 4 Comparison of relative microbial abundance and water chemical content in the three groups of groundwater from Suining, South China

group B and the smallest in group A, while the content of SO_4^{2-} and F^- is the same in the three groups of groundwater. This shows that the relative abundance of Cyanobacteria has the same informational effect as the content of the two water chemistry components. The correlation between the relative abundance of microbial communities and the hydrochemical information in the groundwater environment can be inferred, which reveals that different groundwater environments certainly have corresponding characteristic microbial communities.

The software R version 4.0.2 can be used to quantify the correlation between microbial communities and environmental factors at the species level to obtain deeper-level descriptions and graphics (Fig. 5). *Acinetobacter-radioresistens* (OTU8) and six types of unclassified *Proteobacteria* (OTU 9, 10, 24 and 25) are all positively correlated with pH, EC, HCO_3^- and Ca^{2+}, and there are also unclassified *Proteobacteria* (OTU22) and *Deinococcus-grandis* (OTU18) significantly positively correlated with them. The two unclassified *Proteobacteria* (OTU21 and 64) have a significantly positive correlation with K^+, Cl^-, Mg^{2+}, SiO_2 and a negative correlation with SO_4^{2-} and F^-. The unclassified *Fusobacteria* (OTU35) has a positive correlation with Na^+, SO_4^{2-}, Cl^-, F^-, and Sr. This shows that the microbial communities at species levels also have different correlations at the same phylum level. The three unclassified *Proteobacteria* (OTU3, 7and 15),

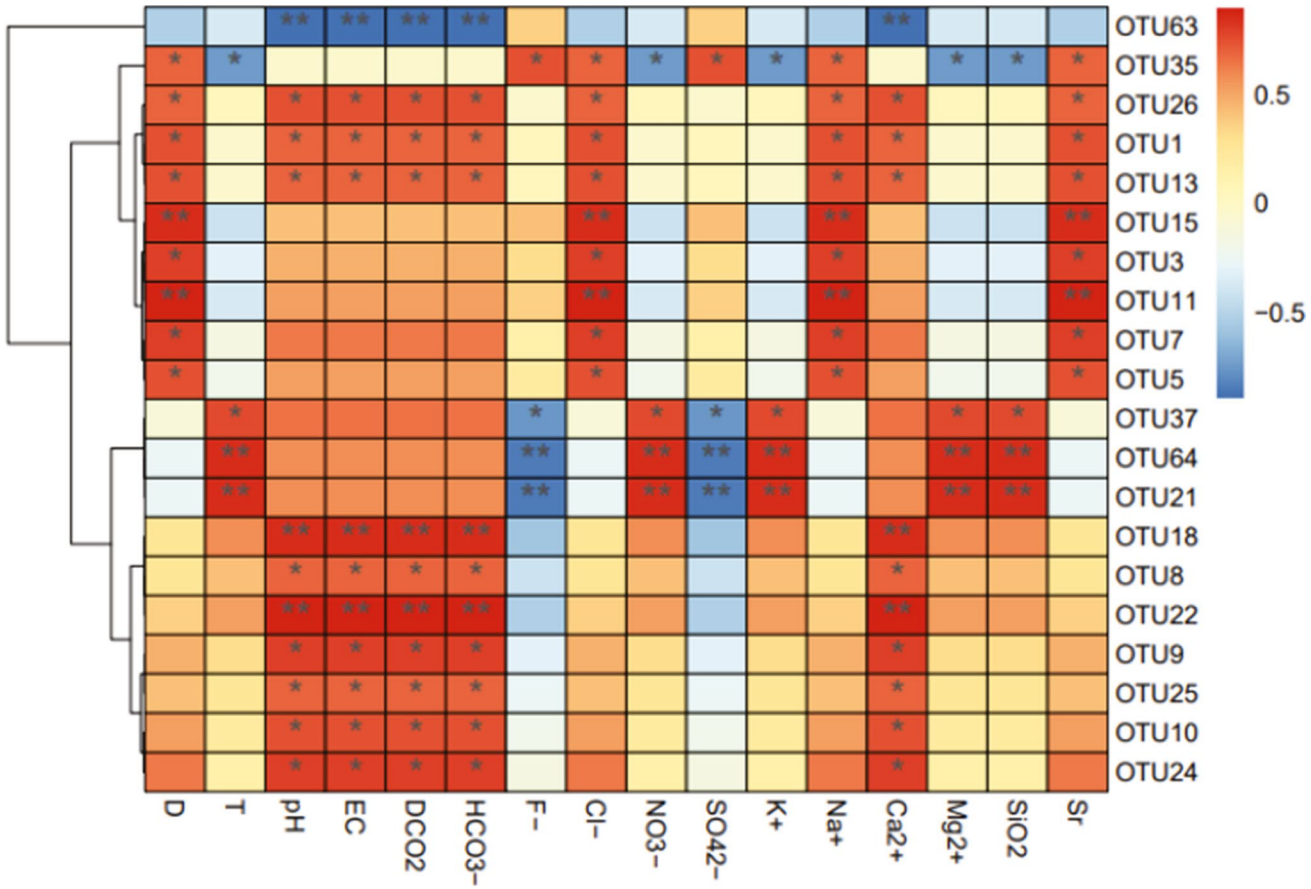

Fig. 5 Heat map analysis of the correlation between environmental factors and the microbial communities (species level) in groundwater samples from Suining, South China

Methylobacterium-radiotolerans (OTU5) and *Actinobacteria* (OTU11) have a positive correlation with Na^+, Cl^- and Sr. This indicates that the content of Na^+, Cl^- in groundwater samples from the study area has a greater impact on the distribution of microbial communities at the species level.

The three groups of groundwater environments with significantly different hydrogeological conditions are revealed by both microbial communities and water chemistry. A microbial community with obvious characteristics can be found in one of the groundwater environments. For example, the relative abundance of Proteobacteria living in group A (deep warm groundwater) with the highest Ca^{2+} and HCO_3^- content is significantly higher than the other two groups. Then, the microbial community can be used as an indicator and tracer, similar to the water chemical composition in the investigation of hydrogeology and groundwater environment.

Mixing evaluation with water chemistry and microbial communities

Based on the hydrochemical composition, the mineral assemblage of water–rock interaction can be inferred (Gonfiantini and Zuppi 2003). The "mineral phases" involved in water–rock interactions in deep warm groundwater at thermal storage temperatures can be inferred by using the Llnl.Dat database of PHREEQC. The dissolution of aragonite, calcite, chalcedony, dolomite, fluorite, halite, K-fledspar, monohydrocalcite, muscovite, pargasite, and tridymite are the main water–rock interactions that influence the chemical composition of deep warm groundwater. However, deep warm groundwater in thermal systems taken from warm-water boreholes (group A) may be mixed with shallow groundwater, from which it is difficult to represent the hydrochemical composition of real deep warm groundwater (Kim et al. 2020). The "mineral phases"

involved in water–rock interactions in deep groundwater using PHREEQC software reach dissolution equilibrium at reservoir temperature, which can be used to simulate the hydrochemical composition of real deep warm groundwater (Parkhurst and Wissmeier 2015). The group C samples (springs) representing the shallow groundwater can be used as a starting point for simulating of water chemistry in deep warm groundwater. According to the hydrogeological conditions of the study area, 11 minerals (including aragonite, calcite, chalcedony, dolomite, small amount of fluorite and halite, K-fledspar, monohydrocalcite, muscovite, pargasite, tridymite) are selected as the appropriate reactants in water–rock interactions.

The simulated chemistry composition of real geothermal water and the groundwater mixing ratio calculated by Eq. (2) are given in Table 3. The average value (46.46%) of the mixing ratio calculated by Cl^-, SO_4^{2-} and Na^+ can be used as the suitable mixing ratio.

According to the correlation between the microbial community (phylum level) and water chemical components, the microbial community may also be a mixing tracer, which can be used to calculate the degree of mixing of the geothermal water with shallow groundwater. The deep warm groundwater mixes with shallow groundwater in the upward migration process, but still maintains the characteristics of geothermal water, which is reflected in the heterogeneity of water chemical composition in the other two groups of groundwater. The microbial community of group A also preserves the indicative role of the chemical information of deep warm groundwater. However, the microbial communities in groups B and C still represent the characteristic environment of deep groundwater and springs because these two groups of groundwater hardly experience mixing. The hydrogeological difference between group A and group B is that group A is heated by geothermal heat. Only two types of microbial communities (Proteobacteria and Chloroflexi) in group A and group B have a high correlation with temperature, which indicates that other microorganisms are relatively weak in response to temperature. Therefore, the remaining microorganisms in group B are equivalent to the microbial communities in the water environment produced by real geothermal water. Based on the results of each microbial community, the mixing ratios calculated by Eq. (2) are listed in Table 4. The three microbial populations of Actinobacteria, Firmicutes, and Fusobacteria are highly correlated with Cl^-, SO_4^{2-} and Na^+ content, indicating that the calculated results of these three microorganisms are significantly suitable in this study area. Actinobacteria and Fusobacteria have a positive correlation with F^- content, indicating that they may have similar effects on the estimation of mixing. However, these two microorganisms are more likely to be affected by the external environment, resulting in deviations in the assessment of the mixing of geothermal water with shallow groundwater. Therefore, the mixing ratio of 44.68% estimated by Firmicutes is considered reasonable for the shallow groundwater mixed with the deep warm groundwater. This result is almost consistent with the results of the water chemistry assessment.

For the characteristics of the microbial community, the species level is more detailed than the phylum level. The 11 most abundant species in the microbial community were selected to calculate the mixing of shallow groundwater with deep geothermal water (Table 5). The mixing ratios obtained by the data of OTU8, OTU22, OTU9, OTU10, and OTU13 are all negative values. These microbial communities are highly correlated with the changeable ions Ca^{2+} and HCO_3^- (Fig. 5), revealing that these microbial communities are susceptible to external disturbances. Therefore, these microbial communities are not suitable as indicators for assessing mixing ratios, and the results obtained by using them are unreasonable. However, the mixing ratios of OTU3, OTU7, and OTU15 are 66.32, 16.20, and 56.46%, respectively. These three microbial communities have a positive correlation with Na^+ and Cl^- content (Fig. 5), which indicates that they can also be used to calculate the mixing ratio in the same way as water chemistry. The average value here is 46.33%, which is close to the calculation result of OTU479 (43.71%).

The proportion of shallow groundwater mixed with deep warm groundwater indicated by microbial tracing at phylum and species levels is about 44.20% (phylum level 44.68%, species level 46.33 or 43.71%), which is close to the water chemical estimation (the average value 46.46%). The three kinds of groundwater environments with significantly different hydrogeological conditions are revealed by both microbial communities and water chemistry. Based on the apparent correlation between microbial communities and chemical components, microbial communities with high

Table 3 The water chemical concentrations of simulated real geothermal water and the mixing ratio estimated by them

Category	HCO_3^-	F^-	Cl^-	NO_3^-	SO_4^{2-}	K^+	Na^+	Ca^{2+}	Mg^{2+}	SiO_2
Simulated real geothermal water (mg/L)	22.941	0.151	1.170	No data	2.035	0.567	11.99	4.524	1.057	35.664
Mixing ratio (%)	–1587.10	286.70	32.78	No data	60.30	125.43	46.30	–919.77	–9.22	–389.46

Table 4 The relative abundance of microorganisms (phylum level) and the mixing ratio of thermal groundwater by shallow groundwater

Category	Acidobacteria	Actinobacteria	Bacteroidetes	Chloroflexi	Cyanobacteria	Deinococcus-Thermus	Firmicutes	Fusobacteria	Planctomycetes	Proteobacteria	Verrucomicrobia
Relative abundance in group A	0.00588	0.06095	0.08899	0.00692	0.00439	0.01479	0.02775	0.00317	0.00767	0.74178	0.00854
Relative abundance in group B	0.00470	0.09010	0.10279	0.02088	0.04957	0.01142	0.04052	0.01852	0.01146	0.60543	0.01085
Relative abundance in group C	0.03531	0.04173	0.17624	0.01490	0.01204	0.00691	0.01194	0.00195	0.05524	0.45741	0.09300
Mixing ratio (%)	3.83	60.26	–18.77	233.62	120.39	–74.72	44.68	92.63	–8.65	–92.12	–2.81

Table 5 The relative abundance of microorganisms (species level) and the mixing ratios estimated by them. *OTU* operational taxonomic unit

Category	OTU1	OTU8	OTU7	OTU3	OTU22	OTU9	OTU41	OTU10	OTU479	OTU15	OTU13
Relative abundance in group A	0.80300	0.14148	0.08259	0.04291	0.07592	0.05228	0.02568	0.06194	0.02418	0.02274	0.03330
Relative abundance in group B	0.82902	0.04257	0.09606	0.10521	0.02580	0.03422	0.03104	0.01046	0.03474	0.04466	0.03196
Relative abundance in group C	0.18176	0.02114	0.01290	0.01128	0.01011	0.01187	0.02146	0.00364	0.01059	0.00584	0.00725
Mixing Ratio (%)	4.02	–461.49	16.20	66.33	–319.47	–80.80	56.00	–755.03	43.71	56.46	–5.46

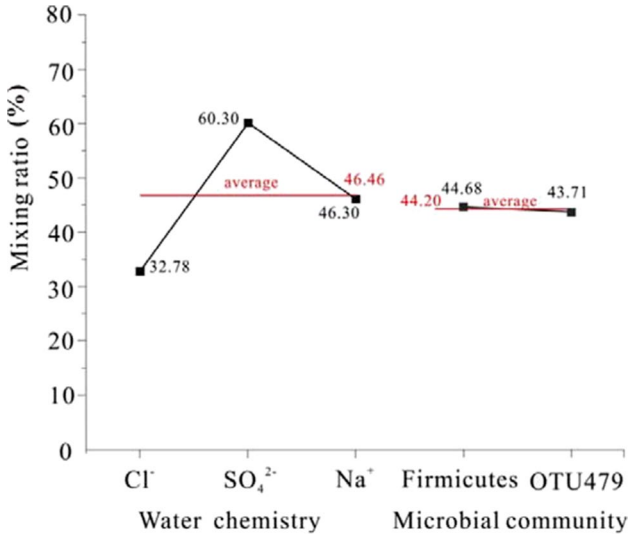

Fig. 6 Groundwater mixing ratios calculated by hydrochemical tracers and microbial tracers in groundwater samples from Suining, South China

correlation with stable chemical components also indicate the good stability of such microbial communities in the processes of groundwater circulation. In Fig. 6, the groundwater mixing ratios calculated by hydrochemical tracers and microbial tracers are basically consistent. This reveals that microbial tracers can be used to calculate the mixing ratio of shallow groundwater mixed with geothermal water, just like water chemistry.

Conclusions

Microbial communities, as well as the water chemistry, were studied to understand the possibility of estimating the degree of mixing of geothermal water and shallow groundwater exposed from the granite fracture network in Suining, South China. According to the hydrogeological conditions and hydrochemical characteristics, the three groups of groundwater have similar hydrochemical types—HCO_3–Na+Ca and HCO_3–Na—but the contents of HCO_3^-, Na^+, Ca^{2+}, and dissolved SiO_2 are different. The three groups of groundwater are of meteoric origin. The deep warm groundwater is 66.5–74.6 °C and it is about 1.93 km deep, with water–rock interactions influencing the main chemical components. The different hydrogeology and geothermal conditions result in different microbial communities in the three types of groundwater. Additionally, the microbial communities are positively correlated with water chemistry at both the phylum and species levels, implying that specific groundwater chemical components lead to specific microbial communities. Three distinct microbial community structures exist in the three different groundwater environments, which can be used to determine the groundwater flow processes, and act as a tracer, much like water chemistry. The simulated chemistry of real geothermal water is used to estimate the mixing ratio of shallow groundwater, and the average value is 46.46%, while the mixing ratio of the shallow groundwater evaluated by the microbial community is 44.68 and 43.71% at the phylum and species level, respectively, whereas their average value is 44.20%. Thus, the microbial communities have the same potential as water chemistry to trace the flow of groundwater and to evaluate the mixing ratio of shallow groundwater and geothermal water.

Acknowledgements Our special thanks go to the editors and three anonymous reviewers for their critical reviews and helpful comments.

Funding This research project was financially supported by the National Natural Science Foundation of China (grant number: 41440027).

Declarations

Conflicts of interest The authors declare that they have no known competing financial interests or personal relationships that could have appeared to influence the work reported in this paper. On behalf of all authors, the corresponding author states that there is no conflict of interest.

References

Al-Qudah O, Woocay A, Walton J (2011) Identification of probable groundwater paths in the Amargosa Desert vicinity. Appl Geochem 26(4):565–574. https://doi.org/10.1016/j.apgeochem.2011.01.014

Arnórsson S, Gunnlaugsson E, Svavarsson H (1983) The chemistry of geothermal waters in Iceland. III. Chemical geothermometry in geothermal investigations. Geochim Cosmochim Acta 47:567–577. https://doi.org/10.1016/0016-7037(83)90278-8

Aydin H, Karakuş H, Mutlu H (2020) Hydrogeochemistry of geothermal waters in eastern Turkey: geochemical and isotopic constraints on water-rock interaction. J Volcanol Geotherm Res 390:106708. https://doi.org/10.1016/j.jvolgeores.2019.106708

Beyer A, Rzanny M, Weist A, Möller S, Burow K, Gutmann F, Neumann S, Lindner J, Müsse S, Brangsch H, Stoiber-Lipp J, Lonschinski M, Merten D, Büchel G, Kothe E (2015) Aquifer community structure in dependence of lithostratigraphy in groundwater reservoirs. Environ Sci Pollut R 22(24):19342–19351. https://doi.org/10.1007/s11356-015-4682-5

Birkle P, García BM, Padrón CMM (2009) Origin and evolution of formation water at the Jujo-Tecominoacán oil reservoir, Gulf of Mexico. Part 1: Chemical evolution and water-rock interaction. Appl Geochem 24(4):543–554. https://doi.org/10.1016/j.apgeochem.2008.12.009

Chae GT, Yun ST, Kim K, Mayer B (2006) Hydrogeochemistry of sodium-bicarbonate type bedrock groundwater in the Pocheon spa area, South Korea: water–rock interaction and hydrologic mixing. J Hydrol 321(1–4):326–343. https://doi.org/10.1016/j.jhydrol.2005.08.006

Fournier RO (1977) Chemical geothermometers and mixing models for geothermal systems. Geothermics 5(1–4):41–50. https://doi.org/10.1016/0375-6505(77)90007-4

Fournier RO, Truesdell AH (1973) An empirical Na-K-Ca geothermometer for natural waters. Geochim Cosmochim Acta 37(5):1255–1275. https://doi.org/10.1016/0016-7037(73)90060-4

Giggenbach WF, Gonfiantini R, Jangi BL, Truesdell AH (1983) Isotopic and chemical composition of Parbati Valley geothermal discharges, North-West Himalaya, India. Geothermics 12(2–3):199–222. https://doi.org/10.1016/0375-6505(83)90030-5

Girmay E, Ayenew T, Kebede S, Alene M, Wohnlich S, Wisotzky F (2015) Conceptual groundwater flow model of the Mekelle Paleozoic-Mesozoic sedimentary outlier and surroundings (northern Ethiopia) using environmental isotopes and dissolved ions. Hydrogeol J 23(4):649–672. https://doi.org/10.1007/s10040-015-1243-4

Gonfiantini R, Zuppi GM (2003) Carbon isotope exchange rate of DIC in karst groundwater. Chem Geol 197(1):319–336. https://doi.org/10.1016/S0009-2541(02)00402-3

Guo L, Wang G, Sheng Y, Shi Z, Sun X (2019) Groundwater microbial communities and their connection to hydrochemical environment in Golmud, Northwest China Sci Total Environ 695:133848. https://doi.org/10.1016/j.scitotenv.2019.133848

Haack S, Fogarty L, West T, Alm E, McGuire J, Long D, Hyndman D, Forney L (2004) Spatial and temporal changes in microbial community structure associated with recharge-influenced chemical gradients in a contaminated aquifer. Environ Microbiol 6(5):438–448. https://doi.org/10.1111/j.1462-2920.2003.00563.x

Hallbeck L, Pedersen K (2011) Culture-dependent comparison of microbial diversity in deep granitic groundwater from two sites considered for a Swedish final repository of spent nuclear fuel. FEMS Microbiol Ecol 81(1):66–77. https://doi.org/10.1111/j.1574-6941.2011.01281.x

Han DM, Liang X, Jin MG, Currell MJ, Song XF, Liu CM (2010) Evaluation of groundwater hydrochemical characteristics and mixing behavior in the Daying and Qicun geothermal systems, Xinzhou Basin. J Volcanol Geotherm Res 189(1–2):92–104. https://doi.org/10.1016/j.jvolgeores.2009.10.011

Haveman SA, Pedersen K (2002) Distribution of culturable microorganisms in Fennoscandian Shield groundwater. FEMS Microbiol Ecol 39(2):129–137. https://doi.org/10.1016/S0168-6496(01)00210-0

Holden JF, Summit M, Baross JA (1998) Thermophilic and hyperthermophilic microorganisms in 3–30 °C hydrothermal fluids following a deep-sea volcanic eruption. FEMS Microbiol Ecol 25(1):33–41. https://doi.org/10.1016/S0168-6496(97)00081-0

Hou Z, Xu T, Li S, Jiang Z, Feng B, Cao Y, Feng G, Yuan Y, Hu Z (2019) Reconstruction of different original water chemical compositions and estimation of reservoir temperature from mixed geothermal water using the method of integrated multicomponent geothermometry: a case study of the Gonghe Basin, northeastern Tibetan Plateau, China. Appl Geochem 108:104389. https://doi.org/10.1016/j.apgeochem.2019.104389

Křoupalová V, Opravilová V, Bojková J, Horsák M (2013) Diversity and assemblage patterns of microorganisms structured by the groundwater chemistry gradient in spring fens. Ann Limnol-Int J Lim 49(3):207–223. https://doi.org/10.1051/limn/2013056

Kim KH, Yun ST, Yu S, Choi BY, Kim MJ, Lee KJ (2020) Geochemical pattern recognitions of deep thermal groundwater in South Korea using self-organizing map: identified pathways of geochemical reaction and mixing. J Hydrol 589:125202. https://doi.org/10.1016/j.jhydrol.2020.125202

Li Y, Pang Z, Yang F, Yuan L, Tang P (2017) Hydrogeochemical characteristics and genesis of the high-temperature geothermal system in the Tashkorgan basin of the Pamir syntax, western China. J Asian Earth Sci 149:134–144. https://doi.org/10.1016/j.jseaes.2017.06.007

Mao X, Wang Y, Zhan H, Feng L (2015) Geochemical and isotopic characteristics of geothermal springs hosted by deep-seated faults in Dongguan Basin, southern China. J Geochem Explor 158:112–121. https://doi.org/10.1016/j.gexplo.2015.07.008

Mao X, Wang H, Feng L (2018) Impact of additional dead carbon on the circulation estimation of thermal springs exposed from deep-seated faults in the Dongguan basin, southern China. J Volcanol Geotherm Res 361:1–11. https://doi.org/10.1016/j.jvolgeores.2018.08.002

Mao X, Zhu D, Ndikubwimana I, He Y, Shi Z (2021) The mechanism of high-salinity thermal groundwater in Xinzhou geothermal field, South China: insight from water chemistry and stable isotopes. J Hydrol 593:1–15. https://doi.org/10.1016/j.jhydrol.2020.125889

Mao X, Dong Y, He Y, Zhu D, Shi Z, Ye J (2022) The effect of granite fracture network on silica-enriched groundwater formation and geothermometers in low-temperature hydrothermal system. J Hydrol 609:127720. https://doi.org/10.1016/j.jhydrol.2022.127720

Marbun BTH, Ridwan RH, Nugraha HS, Sinaga SZ, Purbantanu BA (2020) Casing setting depth and design of production well in water-dominated geothermal system with 330 °C reservoir temperature. Energy Rep 6:582–593. https://doi.org/10.1016/j.egyr.2020.02.013

Modie LT, Kenabatho PK, Stephens M, Mosekiemang T (2022) Investigating groundwater and surface water interactions using stable isotopes and hydrochemistry in the Notwane River Catchment, South East Botswana. J Hydrology: Reg Stud 40:101014. https://doi.org/10.1016/j.ejrh.2022.101014

Mu HM, Wan YY, Wu BC, Tian Y, Dong HL, Xian CG, Li Y (2021) A rapid change in microbial communities of the shale gas drilling fluid from 3548 m depth to the above-ground storage tank. Sci Total Environ 784:147009. https://doi.org/10.1016/j.scitotenv.2021.147009

Ndikubwimana I, Mao X, Zhu D, He Y, Shi Z (2020) Geothermal evolution of deep parent fluid in Western Guangdong, China: evidence from water chemistry, stable isotopes and geothermometry. Hydrogeol J 28(8):2947–2961. https://doi.org/10.1007/s10040-020-02222-x

Nieva D, Nieva R (1987) Developments in geothermal energy in Mexico, part twelve—a cationic geothermometer for prospecting of geothermal resources. Heat Recovery Syst CHP 7(3):243–258. https://doi.org/10.1016/0890-4332(87)90138-4

Park S, Kim HK, Kim MS, Lee GM, Song DH, Jeon SH, Kim Y, Kim TS (2016) Monitoring nitrate natural attenuation and analysis of indigenous micro-organism community in groundwater. Desalin Water Treat 57(51):24096–24108. https://doi.org/10.1080/19443994.2016.1145955

Parkhurst DL, Appelo ZAJ (1999) User's guide to PHREEQC (version 2): a computer program for speciation, batch-reaction, one-dimensional transport, and inverse geochemical calculations. US Geol Surv Water Resour Invest Rep 99(4259):312 http://acamedia.info/sciences/J_G/references/PHREEQC_Manual.pdf

Parkhurst DL, Wissmeier L (2015) PhreeqcRM: a reaction module for transport simulators based on the geochemical model PHREEQC. Adv Water Resour 83:176–189. https://doi.org/10.1016/j.advwatres.2015.06.001

Pérez-Zárate D, Prol-Ledesma RM, Rodríguez-Díaz AA, Jácome-Paz MP, González-Romo IA (2022) Soil gas flux, hydrogeochemistry and multicomponent geothermometry of thermal springs in the La Escalera geothermal prospect, Mexico. Appl Geochem 139:105256. https://doi.org/10.1016/j.apgeochem.2022.105256

Plummer LN (1985) Geochemical modeling: a comparison of forward and inverse methods. In: Proceedings First Canadian/American Conference on Hydrogeology: practical applications of ground water geochemistry. National Water Well Association, Westerville, OH, pp 149–177

Qin D, Turner J, Pang Z (2005) Hydrogeochemistry and groundwater circulation in the Xi'an geothermal field, China. Geothermics 34:471–494. https://doi.org/10.1016/j.geothermics.2005.06.004

Song F, Dong Z, Xu P, Zhou L, Wang S, Duan R (2016) Granite microcracks: structure and connectivity at different depths. J Afr Earth Sci 124:156–168. https://doi.org/10.1016/j.jseaes.2016.04.023

Song B, Zeng Z, Zeng G, Gong J, Xiao R, Chen M, Tang X, Ye S, Shen M (2020) Effects of hydroxyl, carboxyl and amino functionalized carbon nanotubes on the functional diversity of microbial community in riverine sediment. Chemosphere 262:128053. https://doi.org/10.1016/j.chemosphere.2020.128053

Stackebrandt E, Murray RGE, Truper HG (1988) Proteobacteria classis nov, a name for the Phylogenetic Taxon that includes the "purple bacteria and their relatives". Int J Syst Evol Microbiol 38(3):321–325. https://doi.org/10.1099/00207713-38-3-321

Stefánsson A, Arnórsson S, Sveinbjörnsdóttir ÁE, Heinemaier J, Kristmannsdóttir H (2019) Isotope (δD, $\delta^{18}O$, ^{3}H, $\delta^{13}C$, ^{14}C) and chemical (B, Cl) Constrains on water origin, mixing, water–rock interaction and age of low-temperature geothermal water. Appl Geochem 108:104380. https://doi.org/10.1016/j.apgeochem.2019.104380

Stelling P, Shevenell L, Hinz N, Coolbaugh M, Melosh G, Cumming W (2016) Geothermal systems in volcanic arcs: volcanic characteristics and surface manifestations as indicators of geothermal potential and favorability worldwide. J Volcanol Geotherm Res 324:57–72. https://doi.org/10.1016/j.jvolgeores.2016.05.018

Tang X, Zhang J, Pang Z, Hu S, Wu Y, Bao S (2017) Distribution and genesis of the eastern Tibetan Plateau geothermal belt, western China. Environ Earth Sci 76(1):31. https://doi.org/10.1007/s12665-016-6342-6

Wang H, Ni J, Song Q, Li C, Wang F, Cao Y (2021) Analysis of coastal groundwater hydrochemistry evolution based on groundwater flow system division. J Hydrol 601:126631. https://doi.org/10.1016/j.jhydrol.2021.126631

Woolard CR, Irvine R (1994) Biological treatment of hypersaline wastewater by a biofilm of Halophilic Bacteria. Water Environ Res 66:230–235. https://doi.org/10.2175/WER.66.3.8

Wu G, Yang J, Jiang H, Deng Y, Lear G (2019) Distribution of potentially pathogenic bacteria in the groundwater of the Jianghan Plain, central China. Int Biodeterior Biodegradation 143:104711. https://doi.org/10.1016/j.ibiod.2019.05.028

Wu X, Li C, Sun B, Geng F, Gao S, Lv M, Ma X, Li H, Xing L (2020) Groundwater hydrogeochemical formation and evolution in a karst aquifer system affected by anthropogenic impacts. Environ Geochem Health 42(9):2609–2626. https://doi.org/10.1007/s10653-019-00450-z

Xie L, Wang RC, Chen J, Zhu JC (2010) Mineralogical evidence for magmatic and hydrothermal processes in the Qitianling oxidized tin-bearing granite (Hunan, South China): EMP and (MC)-LA-ICPMS investigations of three types of titanite. Chem Geol 276(1–2):53–68. https://doi.org/10.1016/j.chemgeo.2010.05.020

Xue D, Botte J, Baets BD, Accoe F, Angelika N, Taylor P, Cleemput OV, Berglund M, Boeckx P (2009) Present limitations and future prospects of stable isotope methods for nitrate source identification in surface and groundwater. Water Res 43(5):1159–1170. https://doi.org/10.1016/j.watres.2008.12.048

Ye Q, Liu J, Du J, Zhang J (2016) Bacterial diversity in submarine groundwater along the coasts of the Yellow Sea. Front Microbiol 6:1519. https://doi.org/10.3389/fmicb.2015.01519

Yuan J, Xu F, Zheng T (2022) The genesis of saline geothermal groundwater in the coastal area of Guangdong Province: insight from hydrochemical and isotopic analysis. J Hydrol 605:127345. https://doi.org/10.1016/j.jhydrol.2021.127345

Yuan YS, Ma YS, Hu SB, Guo TL, Fu XY (2006) Present day geothermal characteristics in South China. Chin J Geophys 49(4):1005–1014. https://doi.org/10.1002/cjg2.922

Zeng X, Hosono T, Ohta H, Niidome T, Shimada J, Morimura S (2016) Comparison of microbial communities inside and outside of a denitrification hotspot in confined groundwater. Int Biodeterior Biodegrad 114:104–109. https://doi.org/10.1016/j.ibiod.2016.05.019

Zhou Y, Kellermann C, Griebler C (2012) Spatio-temporal patterns of microbial communities in a hydrologically dynamic pristine aquifer. FEMS Microbiol Ecol 81(1):230–242. https://doi.org/10.1111/j.1574-6941.2012.01371.x

Publisher's note Springer Nature remains neutral with regard to jurisdictional claims in published maps and institutional affiliations.

Springer Nature or its licensor holds exclusive rights to this article under a publishing agreement with the author(s) or other rightsholder(s); author self-archiving of the accepted manuscript version of this article is solely governed by the terms of such publishing agreement and applicable law.